Article

Not peer-reviewed version

GlcNAc6ST2/Chst4 Is Essential for the Synthesis of R-10G-Reactive Keratan Sulfate/Sulfated N-acetyllactosamine Oligosaccharides in Mouse Pleural Mesothelium

Yoshiko Takeda-Uchimura , Midori Ikezaki , Tomoya O. Akama , Yoshito Ihara , Fabrice Allain , Kazuchika Nishitsuji , Kenji Uchimura *

Posted Date: 22 December 2023

doi: 10.20944/preprints202312.1732.v1

Keywords: sulfotransferase; keratan sulfate; sialomucin; mesothelium; Muc16

Article

GlcNAc6ST2/Chst4 Is Essential for the Synthesis of R-10G-Reactive Keratan Sulfate/Sulfated *N*-Acetyllactosamine Oligosaccharides in Mouse Pleural Mesothelium

Yoshiko Takeda-Uchimura [1], Midori Ikezaki [2], Tomoya O. Akama [3], Yoshito Ihara [2], Fabrice Allain [1], Kazuchika Nishitsuji [1,2] and Kenji Uchimura [1,*]

[1] Univ. Lille, CNRS, UMR 8576 - UGSF - Unité de Glycobiologie Structurale et Fonctionnelle, Lille, France; yoshiko.uchimura@univ-lille.fr (Y.T.-U.); fabrice.allain@univ-lille.fr (F.A.); kazuchika.nishitsuji@univ-lille.fr (K.N.); kenji.uchimura@univ-lille.fr (K.U.)

[2] Department of Biochemistry, School of Medicine, Wakayama Medical University, Wakayama 641-8509, Japan; nishit@wakayama-med.ac.jp (K.N.); ikezaki@wakayama-med.ac.jp (M.I.); y-ihara@wakayama-med.ac.jp (Y.I.)

[3] Department of Pharmacology, Kansai Medical University, Osaka 570-8506, Japan; akamat@hirakata.kmu.ac.jp (T.-O.A.)

* Correspondence: kenji.uchimura@univ-lille.fr ; +33(0) 20 33 72 39

Abstract: We have recently shown that 6-sulfo sialyl *N*-acetyllactosamine (LacNAc) in *O*-linked glycan recognized by the CL40 antibody is abundant in the pleural mesothelium under physiological conditions, and that these glycans are complementary synthesized by GlcNAc6ST2 (encoded by *Chst4*) and GlcNAc6ST3 (encoded by *Chst5*) in mice. GlcNAc6ST3 is essential for the synthesis of R-10G-positive keratan sulfate (KS) in the brain. The predicted minimum epitope of the R-10G antibody is a dimeric asialo 6-sulfo LacNAc. Whether the R-10G-reactive KS/sulfated LacNAc oligosaccharides are also present in the pleural mesothelium was unknown. If any, the question of which GlcNAc6ST is the responsible enzyme was another issue to be examined as well. Here, we showed that R-10G-reactive glycans are as abundant in the pulmonary pleura as are CL40-reactive glycans, and that GlcNAc6ST3 is only partially involved in the synthesis of these pleural R-10G glycans, unlike in the adult brain. Unexpectedly, GlcNAc6ST2 is essential for the synthesis of R-10G-positive KS/sulfated LacNAc oligosaccharides in the lung pleura. The type of GlcNAc6ST involved in KS glycan biosynthesis and the magnitude of its contribution to the KS synthesis were found to differ among tissues in vivo. We show that GlcNAc6ST2 is required and sufficient for R-10G-reactive KS synthesis in the lung pleura. Interestingly, R-10G immunoreactivity in KSGal6ST (encoded by *Chst1*) and C6st1 (encoded by *Chst3*) double-deficient mouse lungs was markedly increased. Muc16, a mucin molecule, was shown to be a candidate carrier protein for the pleural R-10G-reactive glycans. These results suggested that R-10G-positive KS/sulfated LacNAc oligosaccharides may play a role in mesothelial cell proliferation and differentiation. Further elucidation of the functions of sulfated glycans synthesized by GlcNAc6ST2 and GlcNAc6ST3, such as R-10G and CL40 glycans, in pathological conditions may lead to a better understanding of the underlying mechanisms of the physiopathology of lung mesothelium.

Keywords: sulfotransferase; keratan sulfate; sialomucin; mesothelium; Muc16

1. Introduction

Recently, we reported that sialyl 6-sulfo *N*-acetyllactosamine (sialyl 6-sulfo LacNAc, Neu5Acα2-3Galβ1-4(6S)GlcNAc), a sialylated GlcNAc-6-sulfated glycan recognized by the CL40 antibody [1], is specifically occurred in the mesothelin-positive mesothelium of pulmonary pleura under physiological conditions [2]. Five human members and four of their mouse orthologs represent the GlcNAc-6-sulfotranseferase (GlcNAc6ST) family [3]. We also reported that synthesis of CL40-positive glycans in mouse lung mesothelium requires GlcNAc6ST2 (encoded by *Chst4*) and GlcNAc6ST3 (encoded by *Chst5*), but not GlcNAc6ST1 (encoded by *Chst2*) or GlcNAc6ST4 (encoded by *Chst7*) [2].

 doi:10.20944/preprints202312.1732.v1

GlcNAc6ST2 and GlcNAc6ST3 are complementary to the synthesis of CL40-reactive sialylated sulfated glycans in mouse pleural mesothelium. Since we previously found that GlcNAc6ST3 is essential for the synthesis of cerebral R-10G-positive keratan sulfate (KS) [4] in which the predicted minimum epitope is an asialo 6-sulfo di-LacNAc [5–8], we tested the possibility that R-10G-reactive KS is also present in the pleural mesothelium. The question of which GlcNAc6ST is the responsible enzyme, if any, was examined as well. Here, we found that R-10G-reactive glycans are abundant in the pulmonary pleura as well as observed with the presence of CL40-reactive glycans, and that GlcNAc6ST3 is only partially involved in the synthesis of these pleural R-10G glycans unlike in the adult brain. Remarkably, GlcNAc6ST2 is essential for the synthesis of R-10G-positive KS/sulfated LacNAc oligosaccharides in the lung pleura. The types of GlcNAc6STs involved in KS glycan biosynthesis and the extent of their contribution to the biosynthesis were found to vary among tissues in vivo. We also showed that the GlcNAc6ST2 is sufficient for R-10G-reactive KS synthesis in the lung pleura. In the KSGal6ST (encoded by *Chst1*) and C6st1 (encoded by *Chst3*) double-deficient mice [9], the level of R-10G immunoreactivity in the lung pleura was clearly increased. Muc16, one of the mucin molecules, was shown to be a candidate carrier protein of the R-10G recognition glycan.

2. Results

2.1. R10G-reactive sulfated glycans are abundant in the mouse pleural mesothelium

R-10G recognizes KS and related glycans [4,5,10]. The minimum recognition determinant of R-10G is 6-sulfo di-LacNac, Galβ1–4GlcNAc(6S)β1–3Galβ1–4GlcNAc(±6S) (Figure 1A). We investigated whether R-10G-reactive KS glycan is present in the mouse lung pleura at steady state. We found strong R-10G immunoreactivity in the pleural mesothelium (Figure 1B). These staining signals were co-localized with the staining signals of an antibody against mesothelin, a marker of mesothelial cells lining the lung pleura, but not with the staining signals of an antibody against laminin, a marker of the basement membranes of alveolar epithelium, endothelium and pleura (Figure 1B). Immunostaining with an isotype-matched control (mouse IgG_1) antibody for R-10G gave no specific signals in the pleura (Figure S1). We then asked if R-10G-reactive glycans are *N*-linked or *O*-linked glycans. GlcNAc-containing fractions of mouse lung lobes were obtained with wheat germ agglutinin (WGA)-coated beads. Western blot analysis for the bead-bound material yielded two bands with molecular weights of > 270 kDa immunoreactive for R-10G. Intensities of these bands were not diminished by PNGase F pretreatment (Figure 1C), indicating that R-10G-reactive glycans are found in high-molecular-weight glycoproteins, and that *O*-linked glycans modified with 6-sulfo di-LacNAc are components of these glycoproteins that are present in high density in the pleural mesothelium of the lungs of adult mice.

Preprints (www.preprints.org) | NOT PEER-REVIEWED | Posted: 22 December 2023 doi:10.20944/preprints202312.1732.v1

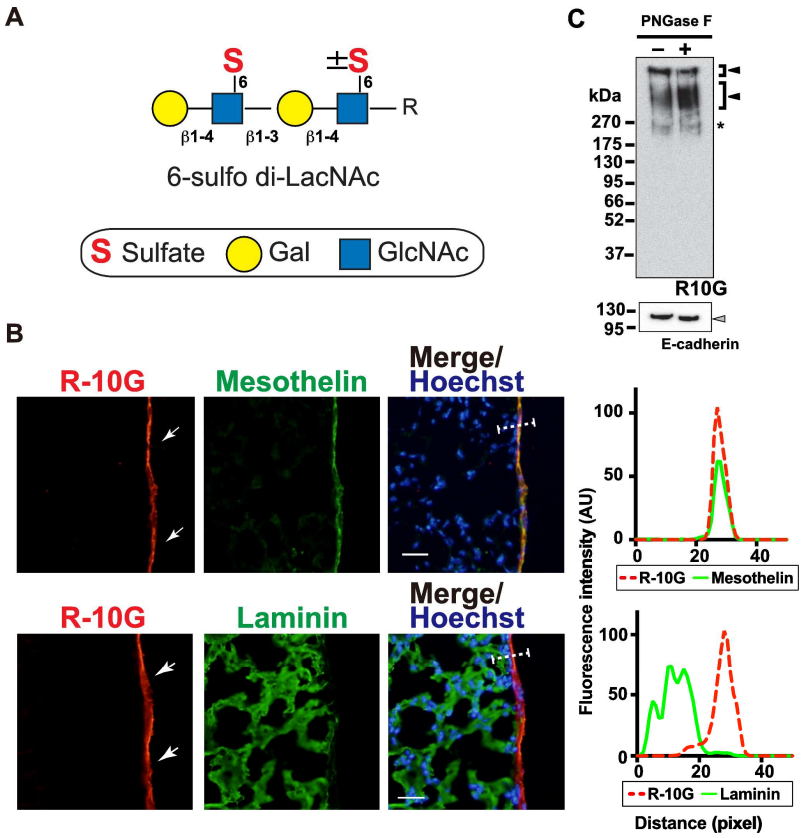

Figure 1. R10G-reactive sulfated glycans are present in the mouse pleural mesothelium. (**A**) Schematic representation of 6-sulfo di-LacNAc recognized by R-10G. C-6 sulfation (S), galactose (Gal), and *N*-acetylglucosamine (GlcNAc) are shown. The glycan is extended from the variable underlying core glycans (R). (**B**) Sections of lungs from normal adult mice were co-stained with R-10G (*red*) and an anti-mesothelin antibody (upper, *green*) or an anti-laminin (lower, *green*), followed by Hoechst 33342 nuclear staining (*blue*). Shown are representative fluorescence microscopy images of the lower and central portions of the left lung lobe (n = 3). Dense R-10G staining signals in the pleural mesothelium (*arrows*) revealed by co-staining with mesothelial marker mesothelin are presented. Plot profiles of R-10G and mesothelin staining or laminin staining are presented. Signal intensities along the line marker (*white dashed line*) paths in the merged images were determined. Scale bar: 20 μm. (**C**) GlcNAc-containing fractions of mouse lung lobes were obtained with wheat germ agglutinin-coated beads. The bead-bound materials were incubated without or with PNGase F. The immunoreactivity of R-10G was tested. Bands with molecular weights of > 270 kDa were observed (*closed arrowheads*). E-cadherin was used to show protein equal loading and successful pretreatment of PNGase F of the lung fraction. The 110 kDa band shifted from 120 kDa in the pretreated fraction (*gray arrowhead*). Bands with 240 kDa were also seen in IgG1 control blots (*asterisk*) [2].

We then investigated whether enzymatic removal of GlcNAc-6-sulfated or non-sulfated poly-LacNAc [11,12] could abolish the R-10G immunoreactivity in the pleura. Pretreatment of lung sections with endo-β-galactosidase could abolish R-10G immunoreactivity (Figure 2A, B). This is consistent with the fact that R-10G epitope requires 6-sulfo di-LacNAc structure as a minimum epitope structure for its recognition [6]. Anti-mesothelin signals were arisen from the mesothelin core protein since these signals were retained after treatment with endo-β-galactosidase (Figure 2A). Next, we wished to determine whether the R10G-reactive glycans were elongated from repeated structure of GlcNAc-6-sulfated and Gal-6-sulfated or non-sulfated disaccharide. Pretreatment of lung sections with keratanase II, which cleaves the sulfated *N*-acetylglucosaminic β1-3 linkage to galactose in non-reducing terminal chain, showed the level of R-10G immunoreactivity comparable to those in enzyme non-treated control (Figure 2A, B). These indicate that R-10G-glycans may be rather short and composed of two LacNAc with GlcNAc-6-sulfation in the non-reducing terminal end of glycans.

Preprints (www.preprints.org) | NOT PEER-REVIEWED | Posted: 22 December 2023 doi:10.20944/preprints202312.1732.v1

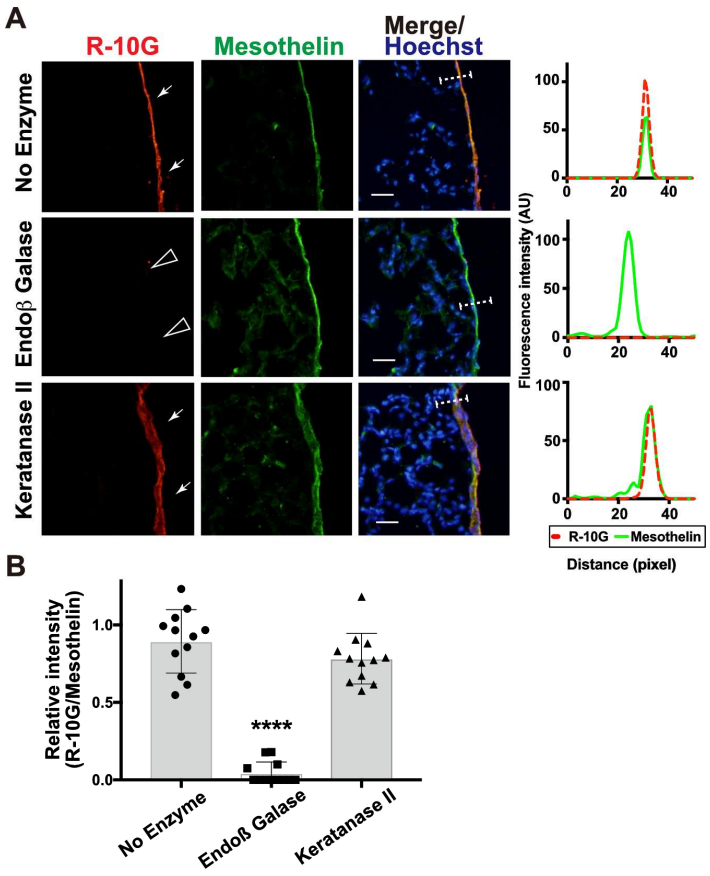

Figure 2. Endo-ß-galactosidase pretreatment diminishes R-10G signals abundant in the mouse pleural mesothelium. (**A**) Sections of lungs from normal adult mice were co-stained with R-10G (*red*) and anti-mesothelin (*green*) followed by Hoechst 33342 nuclear staining (*blue*). Sections were pretreated with buffer only (no enzyme), Endo-β-galactosidase (Endoβ Galase) or Keratanase II, an endo-β-*N*-acetylglucosaminidase. Representative fluorescence microscopy images of the lower and central portions of the left lung lobe are shown (n = 3 per treatment). Dense R-10G staining signals in the pleural mesothelium (*arrows*) revealed by co-staining with an anti-mesothelin are demonstrated. Sections pretreated with Endo-β-galactosidase showed negligible levels of R-10G signals in the mesothelium (*open arrowheads*). Plot profiles of R-10G and mesothelin staining are presented. Signal intensities along the line marker (*white dashed line*) paths in the merged images were determined. (**B**) The relative intensity of R-10G to mesothelin is indicated (n = 12 mesothelium per treatment). Data were obtained from two experiments in which four pleural mesothelium from lung specimens of three donors were analyzed for each genotype. **** $P < 0.0001$. Scale bar: 20 μm.

2.2. GlcNAc6ST2 is required and sufficient for the synthesis of R10G-reactive KS glycans in the mouse pleural mesothelium

We previously showed that 6-sulfo sLe^x present in high endothelial venule (HEV) cells of peripheral lymph nodes is complementarily synthesized by GlcNAc6ST1 and GlcNAc6ST2 [13,14]. Recently, we reported that GlcNAc6ST2 and GlcNAc6ST3 are complement to the synthesis of sialyl 6-sulfo LacNAc recognized by CL40 in mouse pleura [2]. We wished to determine which GlcNAc6ST is responsible for the synthesis of R10G-reactive glycans in mouse pleural mesothelium. We expected that GlcNAc6ST3 might be a major GlcNAc6ST for the pleural R-10G glycans since GlcNAc6ST3 is responsible for R-10G-reactive KS glycans in the brain [4]. Mice genetically deficient in each GlcNAc6ST gene were used for analysis. Mice deficient in GlcNAc6ST1 or GlcNAc6ST4 showed levels comparable to those of WT mice. GlcNAc6ST3-deficient mice showed about 50%-reduced immunoreactivity. This reduction was selectively seen in the area proximal to the basement membrane structure of the mesothelial cell layer. Unexpectedly, mice deficient in GlcNAc6ST2 showed negligible levels of pleural R-10G signals (Figure 3A, B). As seen in the previous report [2],

Preprints (www.preprints.org) | NOT PEER-REVIEWED | Posted: 22 December 2023 doi:10.20944/preprints202312.1732.v1

the mesothelin-positive mesothelium was thickened in GlcNAc6ST2 KO and GlcNAc6ST3 KO mice (Figure 3A). R-10G signals in these KO mice were not colocalized with laminins (Figure S2). These results indicate that both GlcNAc6ST2 and GlcNAc6ST3 are involved in the synthesis of R10G-reactive sulfated glycans in the mouse pleural mesothelium, and that GlcNAc6ST3 is partial but GlcNAc6ST2 is essential for the synthesis. In these KO mice, the mesothelial cell layer may be distorted at the area proximal to the basement membrane for unknown reasons.

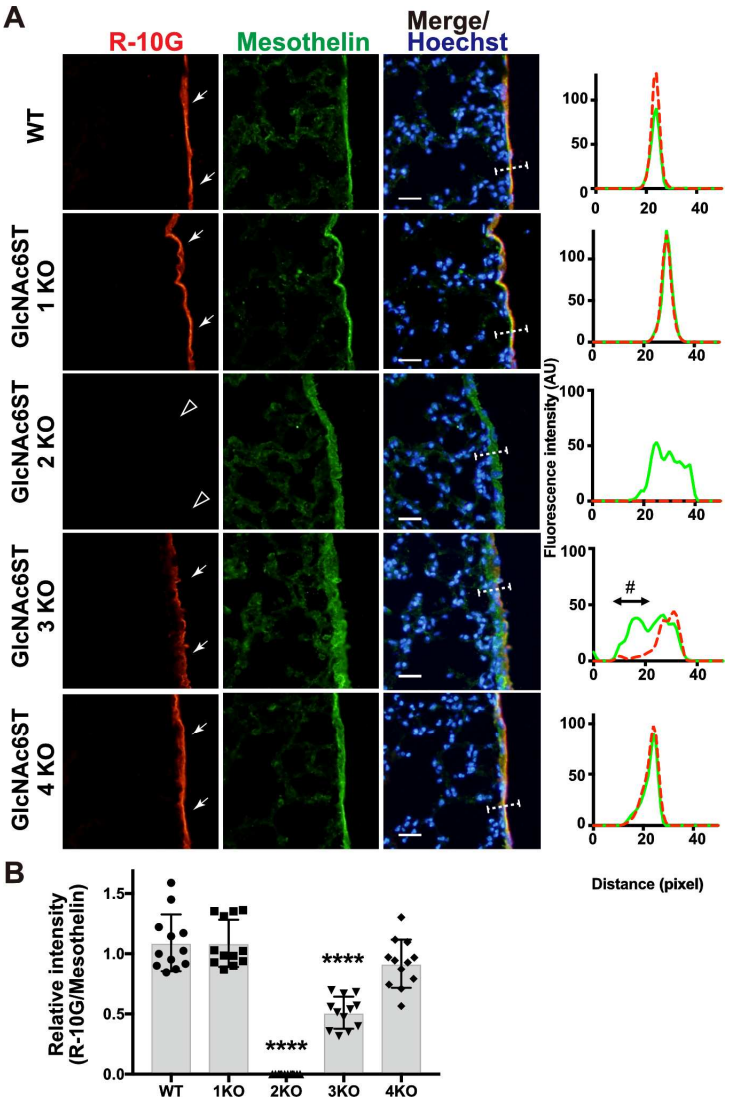

Figure 3. GlcNAc6ST2 is required for synthesis of R-10G-reactive sulfated glycans in mouse pleural mesothelium. (**A**) Sections of lungs from wild-type (WT), *Chst2*-deficient (GlcNAc6ST1 KO) [13,15], *Chst4*-deficient (GlcNAc6ST2 KO) [13,16], *Chst5*-deficient (GlcNAc6ST3 KO) [17], or *Chst7*-deficeint (GlcNAc6ST4 KO) mice [4] were co-stained with R-10G (*red*) and anti-mesothelin (*green*) followed by Hoechst 33342 nuclear staining (*blue*). Dense R-10G staining in the pleural mesothelium is demonstrated (*arrows*). Sections of GlcNAc6ST2 KO showed negligible levels of R-10G signals in the mesothelium (*open arrowheads*) and GlcNAc6ST3 KO mice show reduced levels of R-10G signals. The area proximal to the basement membrane structure in the mesothelial cell layer showed selective reduction in R-10G immunoreactivity (#). Plot profiles of R-10G and mesothelin staining are presented. Signal intensities along the line marker (*white dashed line*) paths in the merged images were determined (n = 3 per genotype). (**B**) The relative intensity of R-10G to mesothelin is indicated (n = 12 mesothelium per genotype). Data were obtained from three experiments in which four pleural mesothelium from lung specimens of three donors were analyzed for each genotype. **** $P < 0.0001$. Scale bar: 20 μm.

Preprints (www.preprints.org) | NOT PEER-REVIEWED | Posted: 22 December 2023 doi:10.20944/preprints202312.1732.v1

We then tested R-10G immunoreactivity in mice triple-deficient (TKO) in GlcNAc6ST1, 3, and 4, but sufficient in GlcNAc6ST2, and mice triple-deficient in GlcNAc6ST1, 2, and 4, but sufficient in GlcNAc6ST3. In agreement with the results of the single KO mice presented above, GlcNAc6ST1, 3 ,4 TKO mice were found to have a significantly reduced level (~30%) of R-10G immunoreactivity. GlcNAc6ST1,2,4 TKO mice showed a negligible level of mesothelial R-10G immunoreactivity (Figure 4A, B), indicating that GlcNAc6ST2 is essential for the synthesis of R-10G KS/KS-related glycans, and that GlcNAc6ST3 has a partial role for the synthesis. These R-10G signals were not colocalized with laminins as seen in single KO lungs (Figure S3).

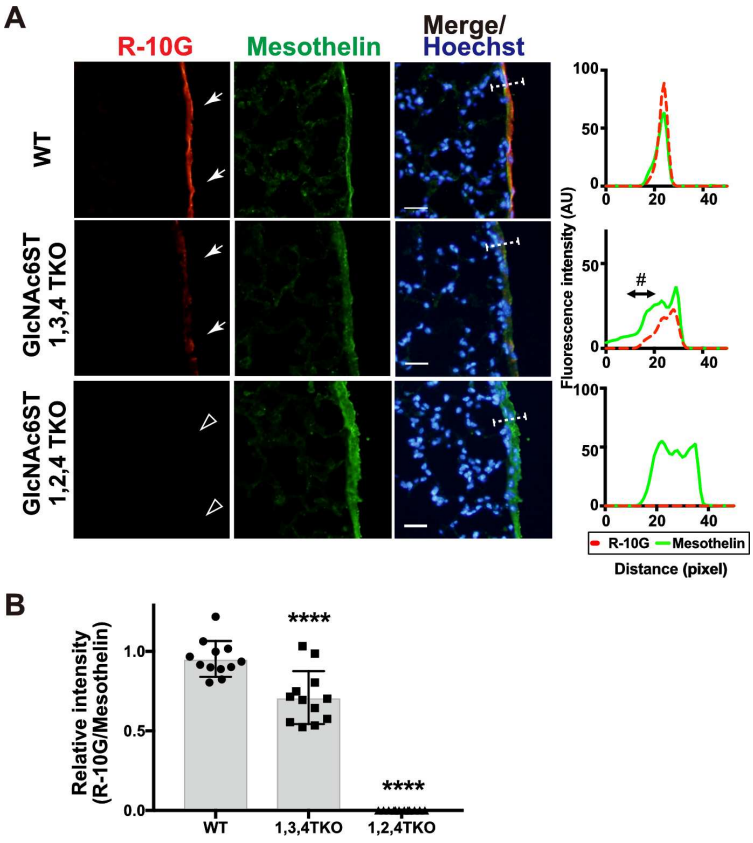

Figure 4. GlcNAc6ST1,2,4 triple KO mice lack R-10G-reactive sulfated glycans in the pleural mesothelium. (**A**) Lung sections prepared from normal wild-type (WT), *Chst2*/*Chst5*/*Chst7* triple-deficient (GlcNAc6ST1,3,4 TKO) and *Chst2*/*Chst4*/*Chst7* triple-deficient (GlcNAc6ST1,2,4 TKO) [18] mice were co-stained with R-10G (*red*) and an anti-mesothelin (*green*) followed by Hoechst 33342 nuclear staining (*blue*). GlcNAc6ST1,2,4 TKO mice showed negligible levels of R-10G signals in the mesothelium (*open arrowheads*). Plot profiles of R-10G and mesothelin staining are presented. Signal intensities along the line marker (*white dashed line*) paths in the merged images were determined (n = 3 per genotype). The area proximal to the basement membrane structure in the mesothelial cell layer showed selective reduction in R-10G immunoreactivity (#). (**B**) The relative intensity of R-10G to mesothelin is indicated (n = 12 mesothelium per genotype). Data were obtained from three experiments in which four pleural mesothelium from lung specimens of three donors were analyzed for each genotype. **** $P < 0.0001$. Scale bar: 20 μm.

KSGal6ST and C6st1 can catalyze the sulfation modification to the 6-position of Gal on KS and related glycans [19–22]. We then asked if double deficiency in these Gal-6-sulfotransferases would change the synthesis and localization of pleural R-10G glycans. We investigated R-10G immunoreactivity in KSGal6ST and C6st1 double knockout mice (DKO) and GlcNAc6ST1, 2 and KSGal6ST TKO mice [9,21]. Western blotting analysis with R-10G showed a band of molecular weight of >250kDa in TBS-soluble fractions (Figure 5A left) and a lower smear band of molecular weights of >250kDa in TBS-insoluble/1% SDS-soluble fractions (Figure 5A right) of lung lysates prepared from

Preprints (www.preprints.org) | NOT PEER-REVIEWED | Posted: 22 December 2023 doi:10.20944/preprints202312.1732.v1

WT and DKO mice, whereas high molecular weight band signals were not observed by the 5D4 anti-Gal-6S, GlcNAc-6S-KS antibody [23] in either fraction of WT and DKO lungs.

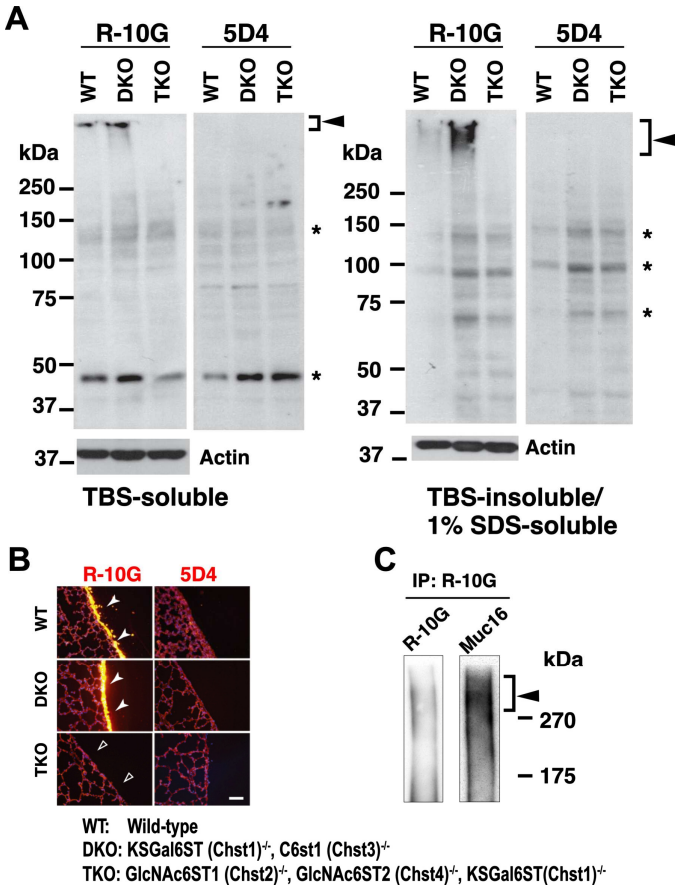

Figure 5. R-10G-immunoreactivity is augmented in the lung of mice double deficient in KSGal6ST and C6st1 and Muc16 in R-10G-immunoprecipitated materials is present. (A) TBS-soluble fraction and TBS-insoluble/1% SDS soluble fraction of lung tissues from normal wild-type (WT), *Chst1*/*Chst3* double-deficient (KSGal6ST/C6st1 DKO) and *Chst2*/*Chst4*/*Chst1* triple-deficient (GlcNAc6ST1,2, and KSGal6ST TKO) [9,21] were prepared. Western blot analysis was performed with R-10G and 5D4. R-10G-reactive bands with molecular weights of > 250 kDa were observed in WT and DKO (*closed arrowheads*). Bands also seen in IgG_1 control blots were indicated (*asterisks*). Note that the intensity of R-10G-immunoreactive band in the DKO TBS-insoluble/1% SDS-soluble fraction is higher than that of WT. (B) Lung sections prepared from WT, KSGal6ST/C6st1 DKO and GlcNAc6ST1,2, and KSGal6ST TKO mice were stained with R-10G (left, *orange*) and 5D4 (right) followed by Hoechst 33342 staining (*blue*). Dense R-10G staining in the pleural mesothelium is shown (*white arrowheads*). The TKO mice showed negligible levels of R-10G signals in the mesothelium (*open arrowheads*). Scale bar: 25 μm. (C) The lung lysates of WT mice were used to prepare R-10G-immunoprecipitated (IP) materials as described in Materials and Methods. IP materials were blotted with R-10G or an anti-Muc16. Smear band with molecular weight of > 270 kDa were observed (*closed arrowhead*). Muc16 was co-precipitated with R-10G-reactive 6-sulfo di-LacNAc.

Interestingly, the intensity of R-10G-immunoreactive band in the DKO TBS-insoluble/1% SDS-soluble fraction was higher than that of WT. In GlcNAc6ST1, 2 and KSGal6ST TKO, these high molecular weight band signals were not observed in either of the two fractions. Therefore, di-LacNAc structures with sulfation modification on both Gal-6 and GlcNAc-6 may not intrinsically exist in the R-10G-reactive glycans. In lung sections of DKO, we observed enhanced R-10G immunoreactivity in the pleura compare to WT mice (Figure 5B left). We did not observe the R-10G signal in GlcNAc6ST1, 2 and KSGal6ST TKO lung sections. 5D4-immunoreactivity in the mouse pleural mesothelium in all genotypes was not observed (Figure 5B right). The scRNA-seq data [24] showed high, selective

Preprints (www.preprints.org) | NOT PEER-REVIEWED | Posted: 22 December 2023 doi:10.20944/preprints202312.1732.v1

expression of *Chst4*, *Msln* and *Muc16* in mesothelial cells (Figure S4). The *Muc16* gene encodes Mucin-16 (Muc16), a highly *O*-glycosylated membrane-associated mucin. Muc16 can be extracellularly released by proteolytic cleavage. We tested if Muc16 is a carrier protein of 6-sulfo di-LacNAc recognized by R-10G. Muc16 was co-immunoprecipitated with R-10G in mouse lung lysates (Figure 5C), indicating that Muc16 could be a candidate molecule carrying R-10G-reactive glycans.

3. Discussion

Recently, we reported that sialyl 6-sulfo LacNAc is complementarily synthesized by GlcNAc6ST2 and GlcNAc6ST3 in the mouse pleura. Here we show that R-10G-reactive KS/KS-related sulfated glycan is also present in the pleural mesothelium and that the R-10G glycan is synthesized essentially by GlcNAc6ST2 in the mouse pleura. We previously showed that synthesis of the R-10G epitope is GlcNAc6ST enzyme-dependent. In the developing brain, GlcNAc6ST1 is one of the major R-10G-reactive glycan synthases [10]. In the adult brain, GlcNAc6ST3 is a major GlcNAc6ST [4,25]. This is the first time, as far as we know, to demonstrate that GlcNAc6ST2 is an enzyme for R-10G-reactive KS/KS-related glycans in vivo.

One possible explanation is that R-10G recognition is reduced to 50% in GlcNAc6ST3 KO mesothelium because of a partial elimination of sulfate group in the recognition epitope of R-10G. As we proposed and summarized in Figure 6, there could be a variation in GlcNAc-6-sulfation of di-LacNAc in the lung pleura. GlcNAc-6-sulfation of the penultimate LacNAc may not be essential for R-10G antibody recognition [6,7]. However, the absence of which may significantly reduce its recognition. GlcNAc-6-sulfation of this penultimate LacNAc is carried by the complementary action of GlcNAc6ST2 and GlcNAc6ST3, whereas GlcNAc-6-sulfation of the non-reducing terminal LacNAc, which is essential for R-10G recognition, may be catalyzed by GlcNAc6ST2 alone (Figure 6). This substrate specificity of GlcNAc6ST2 may explain the R-10G immunostaining phenotype of GlcNAc6ST2 KO and GlcNAc6ST1,3,4 TKO mice. As previously reported for in vitro substrate specificity, the GlcNAc6ST3 enzyme may utilize core 2-branched GlcNAc as a better substrate in the pleura [26]. It is not known whether the glycosyltransferases involved in the synthesis of LacNAc repeats are dependent on this penultimate GlcNAc-6-sulfation. In mucin glycome analysis data, sulfated mono- or di-LacNAc is abundant in the mucin glycans [27]. It is probable that R-10G positive glycan is GlcNAc-6-sulfated dimeric LacNAc without sialic acids at the non-reducing terminal end. The CL40-reactive sialyl 6-sulfo LacNAc may be present in the distinct glycan chains (Figure 6).

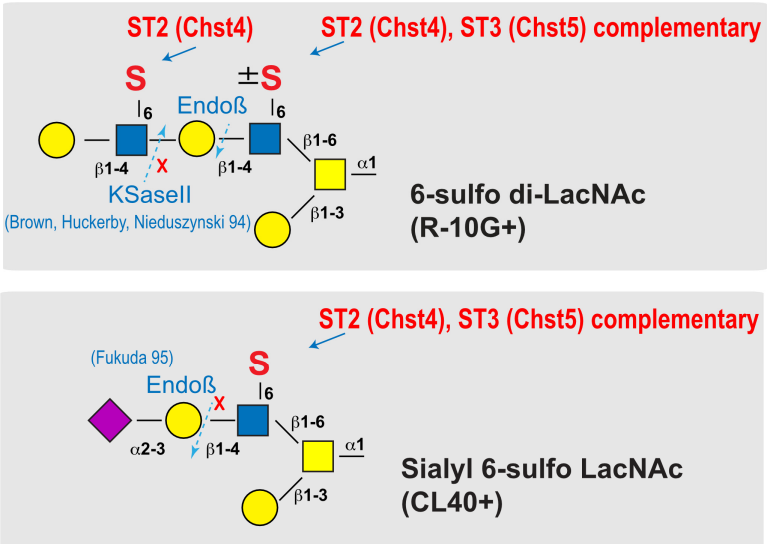

Figure 6. Schematic representation of the reaction mode of GlcNAc6ST2 and GlcNAc6ST3 to 6-sulfo di-LacNAc and sialyl 6-sulfo LacNAc. The mode of synthesis mediated by GlcNAc6ST2 (abbreviated ST2, also known as Chst4) and GlcNAc6ST3 (abbreviated ST3, also known as Chst5) are shown. Predicted susceptibilities to Endo-β-galactosidase (Endoβ) [12] and keratanase II (KSaseII) [28] in

 doi:10.20944/preprints202312.1732.v1

pleural *O*-glycans with asialo 6-sulfo di-LacNAc (Galβ1–4GlcNAc(6S)β1–3Galβ1–4GlcNAc(±6S) or sialyl 6-sulfo LacNAc (Neu5Acα2-3Galβ1-4(6S)GlcNAc) [2] abundant in normal lung are presented. Each symbol denotes: C-6 sulfation (S), galactose (Gal; yellow circle), *N*-acetylglucosamine (GlcNAc; blue square), *N*-acetylgalactosamine (GalNAc; yellow square), and *N*-acetylneuraminic acid, predominant sialic acid (Neu5Ac; purple diamond).

KSGal6ST and C6st1 can catalyze Gal-6-sulfation of KS and related glycans in vivo [9]. 5D4 recognizes KS oligosaccharide structures with absolute dependence on both Gal-6- and GlcNAc-6-sulfation modifications [22,29]. Reactivity of the 5D4 antibody was not observed in mouse lung lobes under physiological conditions, as indicated by biochemical or histological studies. This suggests that KS-containing LacNAc-repeating structures with both Gal-6-sulfation and GlcNAc-6-sulfation are absent or present in very small amounts in the lung mesothelium. One possible reason for the increased R-10G immunoreactivity in the KSGal6ST and C6st1 DKO pleura could be the elevated availability of adenosine 3′-phosphate 5′-phosphosulfate (PAPS; a sulfate donor), to GlcNAc6ST2 and GlcNAc6ST3 in the Golgi complex of mesothelial cells. This may have resulted in an enhanced GlcNAc-6-sulfation reaction and increased R-10G immunoreactivity. KSGal6ST and/or C6st1 may be primarily involved in Gal-6-sulfation of other glycans in mouse mesothelial cells. These glycans may include 6′-sulfo sLex and sialyl 6′-sulfo LacNAc, which can be recognized by mouse sialic acid-binding immunoglobulin-like lectin (Siglec)-F, a paralog of human Siglec-8 [30–35]. The mechanism of region-selective reduction of R-10G immunoreactivity in the GlcNAc6ST3 KO mesothelium is unknown. Whether R-10G-reactive sulfated molecules are different multiple proteins is still remained to be determined. Whether GlcNAc6ST3 is specific to some of the protein species is an issue to be addressed. The possible relationship between sulfated mucin / proteoglycan present in the airways and alveoli [9,36–38] and the mesothelial cell layer in GlcNAc6ST3 deficiency is totally unknown. Because Muc16 is a high binder to mesothelin [39,40] and the encoding gene, *Muc16*, is selectively expressed in mesothelial cells shown by scRNA-seq, Muc16 is a candidate of the R-10G-reactive sulfated molecule in mouse pleura. The shed form of Muc16, known as CA125, promotes cell aggregation and binding to the peritoneal surface through its interaction with mesothelin [39,41]. The possible involvement of GlcNAc-6-sulfation in Muc16 proteolysis and its effect on mesothelin binding or on the recognition of other binding proteins [42] are remained as important issues for the future. The molecular function of Muc16 requires binding partners such as mesothelin, galectin 1, galectin-3, E- and P-selectins [43]. These Muc16-mediated molecular interactions depend on *N*- or *O*-linked glycans [41,43,44]. Given that the R-10G epitope in mouse pleura is predicted to be contained in *O*-linked glycans, our results support a role for the R-10G epitope in determining the interaction between Muc16 modified with R-10G-glycans and its binding partners. Furthermore, glycosylation of Muc16/CA125 is known to differ between physiological and pathological conditions [45]. The regulation of R-10G epitope expression in physiological and disease states requires further elucidation. We found that multiple Hoechst-positive nuclei are abnormally layered in lung pleura of GlcNAc6ST2 KO and GlcNAc6ST3 KO mice. These staining patterns were not observed in WT, GlcNAc6ST1 KO, or GlcNAc6ST4 KO mouse pleural mesothelium. Sulfation modification by GlcNAc6ST2 and GlcNAc6ST3 may play an important role in normal mesothelial layer formation and mesothelial cell proliferation and differentiation. Involvement of these enzymes and enzyme genes in mesothelioma pathogenesis is an interesting topic of research [46]. Exploring the functions of sulfated glycans synthesized by these enzymes, including R-10G and CL40 glycans, in disease states may lead to a better understanding of the pathogenesis of mesothelioma.

4. Materials and Methods

4.1. Antibodies and enzymes

Materials were obtained commercially from the sources indicated as follows. The R-10G anti-GlcNAc-6-sulfo KS antibody was purchased from Cosmo Bio (RIT-M001, Tokyo, Japan); The 5D4 anti-GlcNAc-6-, Gal-6-sulfo KS antibody (MABN2483), mouse anti-β actin (#A2228), and rabbit anti-

 doi:10.20944/preprints202312.1732.v1

laminin antibody (#L9393) were from Sigma-Aldrich (St-Louis, MO, USA); Rabbit anti-mouse mesothelin antibody was from IBL (28127, Fujioka, Japan); Mouse anti E-cadherin antibody was from BD Bioscience (#610182, Franklin Lakes, NJ, USA); Normal mouse IgG_1 was from Santa Cruz (#sc-3877, Dallas, TX, USA). Rabbit anti-Muc16 antibody was from LSBio (#LS-C754876, Shirley, MA, USA). Cy3-conjugated goat anti-mouse IgG_1 (#115-165-205), Alexa Fluor 488-conjugated goat anti-rabbit IgG (H+L) (#111-545-144), HRP-conjugated goat anti-mouse IgG_1 (#115-035-205), HRP-conjugated goat anti-mouse IgG_{2a} (#115-035-206), and HRP-conjugated goat anti-rabbit IgG (H+L) (#111-035-144) were from Jackson ImmunoResearch Laboratories (West Grove, PA, USA); Hoechst33342 was from Dojindo (H342, Kumamoto, Japan). Peptide-N-glycosidase F (PNGase F; P0704S, *Flavobacterium meningosepticum*) was from NEB (Ipswich, MA, USA). Endo-β-galactosidase (#100455, Escherichia freundii) and Keratanase II (#100812, Bacillus sp. Ks 36) were from Seikagaku Corporation (Tokyo, Japan). Enzyme pretreatmets were optimized previously [2,29].

4.2. Mice

GlcNAc6ST1-deficient (KO) [13,15], GlcNAc6ST2-KO [16], GlcNAc6ST3-KO [17], and GlcNAc6ST4-KO mice [4] were maintained on the C57BL/6J genetic background. GlcNAc6ST1,3,4 TKO mice and GlcNAc6ST1,2,4 TKO mice were generated as described previously [4,18]. KSGal6ST [21] / C6st1 [47] double-deficient (DKO), and GlcNAc6ST1,2/KSGal6ST TKO mice were generated by cross-breeding above KO mouse strains [9]. Male and female mice aged 2-4 months were used in the experiments. All mice were maintained under controlled environmental conditions, free of specific pathogens, and provided with standard nutrition and water at the animal housing facilities of the authors' institution.

4.3. Mouse tissues

Mice were anesthetized and transcardially perfused with phosphate buffered saline (PBS). The lung lobes and tracheas were dissected; phosphate buffered solution (PB) containing 4% paraformaldehyde was injected through the airways. Left lung lobes for cryo-sectioning were post-fixed overnight in PB containing 4% paraformaldehyde, equilibrated with 30% sucrose in PBS, and embedded in O.C.T. compound Tissue-Tek (Sakura, Torrance, CA, USA). For biochemical analysis use, the lung tissues were snap-frozen after PBS-perfusion and then stored at −80°C.

4.4. Immunohistochemistry and fluorescence microscopy

Frozen lung tissue was cut into 10-μm-thick sections in a cryostat and collected on MAS-coated glass slides (SF17293; Matsunami, Osaka, Japan). For pre-treatment, the sections were digested with 10 mU/ml endo-ß-galactosidase, or 50 mU/ml Keratanase II in 50 mM Tris-acetate buffer pH 7.0 at 37 °C for 24 h. The sections were stained with R-10G (10 μg/ml) and anti-mesothelin (1:200 dilution) as described previously. Signals were acquired using a fluorescence microscope (BX41; Olympus, Tokyo, Japan) with the same exposure settings for each antibody staining. The fluorescence intensities of Cy3-R10G and Alexa Fluor 488-mesothelin in stained pleura in digital images were determined semiquantitatively using ImageJ (NIH, Bethesda, MD). Four pleural mesothelium per mouse were randomly selected. Three mice were tested for each genotype or treatment.

4.5. Immunoprecipitation

One % Triton X 100-soluble fractions were prepared from tissue homogenates of 100 mg lung lobes of 2- to 3-month-old C57BL/6J mice. The lung lysate was mixed with a complex of the R-10G anti-KS antibody and Protein G Dynabeads (Thermo Fisher Scientific, Waltham, MA, USA) in PB containing 0.02% Tween-20 (PB-T) for 30 min at room temperature. The immunocomplexes bound to the Protein G Dynabeads were isolated with the DynaMag-2 Magnet (Thermo Fisher Scientific).

4.6. WGA bead-bound precipitation

One % Triton X 100-soluble fractions were prepared as described above. The fractions were incubated with GlcNAc-binding WGA-coated beads (Vector Laboratories) at 4 °C overnight. Bead-bound materials were used for Western blot analysis.

4.7. Immunoblots

Frozen lung tissues were homogenized in Tris buffered saline (TBS) with protease inhibitors as previously described [48]. The tubes were subsequently placed in a Bioruptor sonicator water bath (Cosmo Bio, Inc.). The tissue was crushed 4-5 times for 15 seconds at maximum ultrasound power until no solids were visible in the tubes. The tissue was then ultracentrifuged at 100,000 x g for 30 minutes at 4°C. The supernatant fluid was collected (TBS-soluble fraction). The pellet was suspended in TBS contained 1% SDS, and the pellet was dissociated and centrifuged at 15,000 × *g* for 20 minutes at room temperature. The supernatant fluid was collected (TBS-insoluble/1% SDS-soluble fraction). Immunoblotting was performed as described previously [29] with the following antibody concentrations: R-10G anti-KS (dilution 1:1000), 5D4 anti-KS (1:1000), anti-E-cadherin (1:1000), HRP-conjugated goat anti-mouse IgG1 secondary antibody (1:3000), goat anti-rabbit IgG (1:1000), goat anti mouse IgG2a (1:5000).

4.8. Statistical analysis

All data are presented as means ± SE unless otherwise noted. The values were analyzed by one-way analysis of variance with Dunnett's test (vs wild-type or without enzyme control) with Prism (GraphPad Software, La Jolla, CA). P-values less than 0.05 were considered statistically significant.

Author Contributions: Y.T-U., M.I., K.N, and K.U. performed experiments. Y.T-U., K.N., and K.U. interpreted data and wrote the manuscript. T.O.A., F.A. and Y.I. contributed resources.

Supplementary Materials: The following supporting information can be downloaded at the website of this paper posted on Preprints.org.

Acknowledgments: We are grateful to Steven D. Rosen and Michael L. Patnode for providing frozen tissues of KSGal6ST and C6st1 double-deficient mice and GlcNAc6ST1, 2, and KSGal6ST triple- deficient mice.

Conflicts of Interest: The authors declare no potential conflicts of interest with respect to the authorship or publication of this article.

References

1. Arata-Kawai, H.; Singer, M.S.; Bistrup, A.; Zante, A.; Wang, Y.Q.; Ito, Y.; Bao, X.; Hemmerich, S.; Fukuda, M.; Rosen, S.D. Functional contributions of N- and O-glycans to L-selectin ligands in murine and human lymphoid organs. *Am J Pathol* **2011**, *178*, 423-433, doi:10.1016/j.ajpath.2010.11.009.
2. Takeda-Uchimura, Y.; Ikezaki, M.; Akama, T.O.; Nishioka, K.; Ihara, Y.; Allain, F.; Nishitsuji, K.; Uchimura, K. Complementary Role of GlcNAc6ST2 and GlcNAc6ST3 in Synthesis of CL40-Reactive Sialylated and Sulfated Glycans in the Mouse Pleural Mesothelium. *Molecules* **2022**, *27*, doi:10.3390/molecules27144543.
3. Uchimura, K.; Rosen, S.D. Sulfated L-selectin ligands as a therapeutic target in chronic inflammation. *Trends Immunol* **2006**, *27*, 559-565, doi:10.1016/j.it.2006.10.007.
4. Narentuya; Takeda-Uchimura, Y.; Foyez, T.; Zhang, Z.; Akama, T.O.; Yagi, H.; Kato, K.; Komatsu, Y.; Kadomatsu, K.; Uchimura, K. GlcNAc6ST3 is a keratan sulfate sulfotransferase for the protein-tyrosine phosphatase PTPRZ in the adult brain. *Sci Rep* **2019**, *9*, 4387, doi:10.1038/s41598-019-40901-2.
5. Kawabe, K.; Tateyama, D.; Toyoda, H.; Kawasaki, N.; Hashii, N.; Nakao, H.; Matsumoto, S.; Nonaka, M.; Matsumura, H.; Hirose, Y.; et al. A novel antibody for human induced pluripotent stem cells and embryonic stem cells recognizes a type of keratan sulfate lacking oversulfated structures. *Glycobiology* **2013**, *23*, 322-336, doi:10.1093/glycob/cws159.
6. Nakao, H.; Nagai, Y.; Kojima, A.; Toyoda, H.; Kawasaki, N.; Kawasaki, T. Binding specificity of R-10G and TRA-1-60/81, and substrate specificity of keratanase II studied with chemically synthesized oligosaccharides. *Glycoconj J* **2017**, *34*, 789-795, doi:10.1007/s10719-017-9765-8.

7. Wu, N.; Silva, L.M.; Liu, Y.; Zhang, Y.; Gao, C.; Zhang, F.; Fu, L.; Peng, Y.; Linhardt, R.; Kawasaki, T.; et al. Glycan Markers of Human Stem Cells Assigned with Beam Search Arrays. *Mol Cell Proteomics* **2019**, *18*, 1981-2002, doi:10.1074/mcp.RA119.001309.
8. Nakao, H.; Yamaguchi, T.; Kawabata, K.; Higashi, K.; Nonaka, M.; Tuiji, M.; Nagai, Y.; Toyoda, H.; Yamaguchi, Y.; Kawasaki, N.; et al. Characterization of novel antibodies that recognize sialylated keratan sulfate and lacto-N-fucopentaose I on human induced pluripotent cells: comparison with existing antibodies. *Glycobiology* **2023**, *33*, 150-164, doi:10.1093/glycob/cwac074.
9. Patnode, M.L.; Cheng, C.W.; Chou, C.C.; Singer, M.S.; Elin, M.S.; Uchimura, K.; Crocker, P.R.; Khoo, K.H.; Rosen, S.D. Galactose 6-O-sulfotransferases are not required for the generation of Siglec-F ligands in leukocytes or lung tissue. *J Biol Chem* **2013**, *288*, 26533-26545, doi:10.1074/jbc.M113.485409.
10. Takeda-Uchimura, Y.; Uchimura, K.; Sugimura, T.; Yanagawa, Y.; Kawasaki, T.; Komatsu, Y.; Kadomatsu, K. Requirement of keratan sulfate proteoglycan phosphacan with a specific sulfation pattern for critical period plasticity in the visual cortex. *Exp Neurol* **2015**, *274*, 145-155, doi:10.1016/j.expneurol.2015.08.005.
11. Fukuda, M.N.; Matsumura, G. Endo-beta-galactosidase of Escherichia freundii. Purification and endoglycosidic action on keratan sulfates, oligosaccharides, and blood group active glycoprotein. *J Biol Chem* **1976**, *251*, 6218-6225.
12. Fukuda, M.N. Endo-β-Galactosidases and Keratanase. *Current Protocols in Molecular Biology* **1995**, *32*, 17.17.16-17.17.13, doi:https://doi.org/10.1002/0471142727.mb1717bs32.
13. Uchimura, K.; Gauguet, J.M.; Singer, M.S.; Tsay, D.; Kannagi, R.; Muramatsu, T.; von Andrian, U.H.; Rosen, S.D. A major class of L-selectin ligands is eliminated in mice deficient in two sulfotransferases expressed in high endothelial venules. *Nat Immunol* **2005**, *6*, 1105-1113, doi:10.1038/ni1258.
14. Kawashima, H.; Petryniak, B.; Hiraoka, N.; Mitoma, J.; Huckaby, V.; Nakayama, J.; Uchimura, K.; Kadomatsu, K.; Muramatsu, T.; Lowe, J.B.; et al. N-acetylglucosamine-6-O-sulfotransferases 1 and 2 cooperatively control lymphocyte homing through L-selectin ligand biosynthesis in high endothelial venules. *Nat Immunol* **2005**, *6*, 1096-1104, doi:10.1038/ni1259.
15. Uchimura, K.; Kadomatsu, K.; El-Fasakhany, F.M.; Singer, M.S.; Izawa, M.; Kannagi, R.; Takeda, N.; Rosen, S.D.; Muramatsu, T. N-acetylglucosamine 6-O-sulfotransferase-1 regulates expression of L-selectin ligands and lymphocyte homing. *J Biol Chem* **2004**, *279*, 35001-35008, doi:10.1074/jbc.M404456200.
16. Hemmerich, S.; Bistrup, A.; Singer, M.S.; van Zante, A.; Lee, J.K.; Tsay, D.; Peters, M.; Carminati, J.L.; Brennan, T.J.; Carver-Moore, K.; et al. Sulfation of L-selectin ligands by an HEV-restricted sulfotransferase regulates lymphocyte homing to lymph nodes. *Immunity* **2001**, *15*, 237-247.
17. Hayashida, Y.; Akama, T.O.; Beecher, N.; Lewis, P.; Young, R.D.; Meek, K.M.; Kerr, B.; Hughes, C.E.; Caterson, B.; Tanigami, A.; et al. Matrix morphogenesis in cornea is mediated by the modification of keratan sulfate by GlcNAc 6-O-sulfotransferase. *Proc Natl Acad Sci U S A* **2006**, *103*, 13333-13338, doi:10.1073/pnas.0605441103.
18. Jiang, L.; Jung, S.; Zhao, J.; Kasinath, V.; Ichimura, T.; Joseph, J.; Fiorina, P.; Liss, A.S.; Shah, K.; Annabi, N.; et al. Simultaneous targeting of primary tumor, draining lymph node, and distant metastases through high endothelial venule-targeted delivery. *Nano Today* **2021**, *36*, doi:10.1016/j.nantod.2020.101045.
19. Habuchi, O.; Hirahara, Y.; Uchimura, K.; Fukuta, M. Enzymatic sulfation of galactose residue of keratan sulfate by chondroitin 6-sulfotransferase. *Glycobiology* **1996**, *6*, 51-57.
20. Fukuta, M.; Inazawa, J.; Torii, T.; Tsuzuki, K.; Shimada, E.; Habuchi, O. Molecular cloning and characterization of human keratan sulfate Gal-6-sulfotransferase. *J Biol Chem* **1997**, *272*, 32321-32328.
21. Patnode, M.L.; Yu, S.Y.; Cheng, C.W.; Ho, M.Y.; Tegesjo, L.; Sakuma, K.; Uchimura, K.; Khoo, K.H.; Kannagi, R.; Rosen, S.D. KSGal6ST generates galactose-6-O-sulfate in high endothelial venules but does not contribute to L-selectin-dependent lymphocyte homing. *Glycobiology* **2013**, *23*, 381-394, doi:10.1093/glycob/cws166.
22. Hoshino, H.; Foyez, T.; Ohtake-Niimi, S.; Takeda-Uchimura, Y.; Michikawa, M.; Kadomatsu, K.; Uchimura, K. KSGal6ST is essential for the 6-sulfation of galactose within keratan sulfate in early postnatal brain. *J Histochem Cytochem* **2014**, *62*, 145-156, doi:10.1369/0022155413511619.
23. Caterson, B.; Christner, J.E.; Baker, J.R. Identification of a monoclonal antibody that specifically recognizes corneal and skeletal keratan sulfate. Monoclonal antibodies to cartilage proteoglycan. *The Journal of biological chemistry* **1983**, *258*, 8848-8854.

24. Angelidis, I.; Simon, L.M.; Fernandez, I.E.; Strunz, M.; Mayr, C.H.; Greiffo, F.R.; Tsitsiridis, G.; Ansari, M.; Graf, E.; Strom, T.M.; et al. An atlas of the aging lung mapped by single cell transcriptomics and deep tissue proteomics. *Nat Commun* **2019**, *10*, 963, doi:10.1038/s41467-019-08831-9.
25. Takeda-Uchimura, Y.; Nishitsuji, K.; Ikezaki, M.; Akama, T.O.; Ihara, Y.; Allain, F.; Uchimura, K. Beta3Gn-T7 Is a Keratan Sulfate beta1,3 N-Acetylglucosaminyltransferase in the Adult Brain. *Front Neuroanat* **2022**, *16*, 813841, doi:10.3389/fnana.2022.813841.
26. Uchimura, K.; El-Fasakhany, F.M.; Hori, M.; Hemmerich, S.; Blink, S.E.; Kansas, G.S.; Kanamori, A.; Kumamoto, K.; Kannagi, R.; Muramatsu, T. Specificities of N-acetylglucosamine-6-O-sulfotransferases in relation to L-selectin ligand synthesis and tumor-associated enzyme expression. *J Biol Chem* **2002**, *277*, 3979-3984, doi:10.1074/jbc.M106587200.
27. Werlang, C.A.; Chen, W.G.; Aoki, K.; Wheeler, K.M.; Tymm, C.; Mileti, C.J.; Burgos, A.C.; Kim, K.; Tiemeyer, M.; Ribbeck, K. Mucin O-glycans suppress quorum-sensing pathways and genetic transformation in Streptococcus mutans. *Nat Microbiol* **2021**, *6*, 574-583, doi:10.1038/s41564-021-00876-1.
28. Brown, G.M.; Huckerby, T.N.; Nieduszynski, I.A. Oligosaccharides derived by keratanase II digestion of bovine articular cartilage keratan sulphates. *Eur J Biochem* **1994**, *224*, 281-308, doi:10.1111/j.1432-1033.1994.00281.x.
29. Foyez, T.; Takeda-Uchimura, Y.; Ishigaki, S.; Narentuya; Zhang, Z.; Sobue, G.; Kadomatsu, K.; Uchimura, K. Microglial keratan sulfate epitope elicits in central nervous tissues of transgenic model mice and patients with amyotrophic lateral sclerosis. *Am J Pathol* **2015**, *185*, 3053-3065, doi:10.1016/j.ajpath.2015.07.016.
30. Bochner, B.S.; Alvarez, R.A.; Mehta, P.; Bovin, N.V.; Blixt, O.; White, J.R.; Schnaar, R.L. Glycan array screening reveals a candidate ligand for Siglec-8. *J Biol Chem* **2005**, *280*, 4307-4312, doi:10.1074/jbc.M412378200.
31. Tateno, H.; Crocker, P.R.; Paulson, J.C. Mouse Siglec-F and human Siglec-8 are functionally convergent paralogs that are selectively expressed on eosinophils and recognize 6'-sulfo-sialyl Lewis X as a preferred glycan ligand. *Glycobiology* **2005**, *15*, 1125-1135, doi:10.1093/glycob/cwi097.
32. Propster, J.M.; Yang, F.; Rabbani, S.; Ernst, B.; Allain, F.H.; Schubert, M. Structural basis for sulfation-dependent self-glycan recognition by the human immune-inhibitory receptor Siglec-8. *Proc Natl Acad Sci U S A* **2016**, *113*, E4170-4179, doi:10.1073/pnas.1602214113.
33. Bull, C.; Nason, R.; Sun, L.; Van Coillie, J.; Madriz Sorensen, D.; Moons, S.J.; Yang, Z.; Arbitman, S.; Fernandes, S.M.; Furukawa, S.; et al. Probing the binding specificities of human Siglecs by cell-based glycan arrays. *Proc Natl Acad Sci U S A* **2021**, *118*, doi:10.1073/pnas.2026102118.
34. Jung, J.; Enterina, J.R.; Bui, D.T.; Mozaneh, F.; Lin, P.H.; Nitin; Kuo, C.W.; Rodrigues, E.; Bhattacherjee, A.; Raeisimakiani, P.; et al. Carbohydrate Sulfation As a Mechanism for Fine-Tuning Siglec Ligands. *ACS Chem Biol* **2021**, *16*, 2673-2689, doi:10.1021/acschembio.1c00501.
35. Wu, Y.; Vos, G.M.; Huang, C.; Chapla, D.; Kimpel, A.L.M.; Moremen, K.W.; de Vries, R.P.; Boons, G.-J. Exploiting Substrate Specificities of 6-O-Sulfotransferases to Enzymatically Synthesize Keratan Sulfate Oligosaccharides. *JACS Au* **2023**, doi:10.1021/jacsau.3c00488.
36. Kiwamoto, T.; Katoh, T.; Evans, C.M.; Janssen, W.J.; Brummet, M.E.; Hudson, S.A.; Zhu, Z.; Tiemeyer, M.; Bochner, B.S. Endogenous airway mucins carry glycans that bind Siglec-F and induce eosinophil apoptosis. *J Allergy Clin Immunol* **2015**, *135*, 1329-1340 e1329, doi:10.1016/j.jaci.2014.10.027.
37. Gonzalez-Gil, A.; Porell, R.N.; Fernandes, S.M.; Wei, Y.; Yu, H.; Carroll, D.J.; McBride, R.; Paulson, J.C.; Tiemeyer, M.; Aoki, K.; et al. Sialylated keratan sulfate proteoglycans are Siglec-8 ligands in human airways. *Glycobiology* **2018**, *28*, 786-801, doi:10.1093/glycob/cwy057.
38. Gonzalez-Gil, A.; Li, T.A.; Porell, R.N.; Fernandes, S.M.; Tarbox, H.E.; Lee, H.S.; Aoki, K.; Tiemeyer, M.; Kim, J.; Schnaar, R.L. Isolation, identification, and characterization of the human airway ligand for the eosinophil and mast cell immunoinhibitory receptor Siglec-8. *J Allergy Clin Immunol* **2021**, *147*, 1442-1452, doi:10.1016/j.jaci.2020.08.001.
39. Kaneko, O.; Gong, L.; Zhang, J.; Hansen, J.K.; Hassan, R.; Lee, B.; Ho, M. A binding domain on mesothelin for CA125/MUC16. *J Biol Chem* **2009**, *284*, 3739-3749, doi:10.1074/jbc.M806776200.
40. Rump, A.; Morikawa, Y.; Tanaka, M.; Minami, S.; Umesaki, N.; Takeuchi, M.; Miyajima, A. Binding of ovarian cancer antigen CA125/MUC16 to mesothelin mediates cell adhesion. *J Biol Chem* **2004**, *279*, 9190-9198, doi:10.1074/jbc.M312372200.
41. Gubbels, J.A.; Belisle, J.; Onda, M.; Rancourt, C.; Migneault, M.; Ho, M.; Bera, T.K.; Connor, J.; Sathyanarayana, B.K.; Lee, B.; et al. Mesothelin-MUC16 binding is a high affinity, N-glycan dependent

interaction that facilitates peritoneal metastasis of ovarian tumors. *Mol Cancer* **2006**, *5*, 50, doi:10.1186/1476-4598-5-50.

42. Belisle, J.A.; Horibata, S.; Jennifer, G.A.; Petrie, S.; Kapur, A.; Andre, S.; Gabius, H.J.; Rancourt, C.; Connor, J.; Paulson, J.C.; et al. Identification of Siglec-9 as the receptor for MUC16 on human NK cells, B cells, and monocytes. *Mol Cancer* **2010**, *9*, 118, doi:10.1186/1476-4598-9-118.
43. Das, S.; Batra, S.K. Understanding the Unique Attributes of MUC16 (CA125): Potential Implications in Targeted Therapy. *Cancer Res* **2015**, *75*, 4669-4674, doi:10.1158/0008-5472.CAN-15-1050.
44. Hanson, R.L.; Hollingsworth, M.A. Functional Consequences of Differential O-glycosylation of MUC1, MUC4, and MUC16 (Downstream Effects on Signaling). *Biomolecules* **2016**, *6*, doi:10.3390/biom6030034.
45. Saldova, R.; Struwe, W.B.; Wynne, K.; Elia, G.; Duffy, M.J.; Rudd, P.M. Exploring the glycosylation of serum CA125. *Int J Mol Sci* **2013**, *14*, 15636-15654, doi:10.3390/ijms140815636.
46. Nakashima, K.; Sakai, Y.; Hoshino, H.; Umeda, Y.; Kawashima, H.; Sekido, Y.; Ishizuka, T.; Kobayashi, M. Sulfated Glycans Recognized by S1 Monoclonal Antibody can Serve as a Diagnostic Marker for Malignant Pleural Mesothelioma. *Lung* **2022**, *200*, 339-346, doi:10.1007/s00408-022-00531-4.
47. Uchimura, K.; Kadomatsu, K.; Nishimura, H.; Muramatsu, H.; Nakamura, E.; Kurosawa, N.; Habuchi, O.; El-Fasakhany, F.M.; Yoshikai, Y.; Muramatsu, T. Functional analysis of the chondroitin 6-sulfotransferase gene in relation to lymphocyte subpopulations, brain development, and oversulfated chondroitin sulfates. *J Biol Chem* **2002**, *277*, 1443-1450, doi:10.1074/jbc.M104719200.
48. Hosono-Fukao, T.; Ohtake-Niimi, S.; Hoshino, H.; Britschgi, M.; Akatsu, H.; Hossain, M.M.; Nishitsuji, K.; van Kuppevelt, T.H.; Kimata, K.; Michikawa, M.; et al. Heparan sulfate subdomains that are degraded by Sulf accumulate in cerebral amyloid ss plaques of Alzheimer's disease: evidence from mouse models and patients. *Am J Pathol* **2012**, *180*, 2056-2067, doi:10.1016/j.ajpath.2012.01.015.